JOURNAL OF SOLID STATE CHEMISTRY 28, 259–268 (1979)

The Formation of a Series of Barium Tungsten Bronzes

THOMMY EKSTRÖM* AND R. J. D. TILLEY†

*Department of Inorganic Chemistry, Arrhenius Laboratory, University of Stockholm, S-106 91 Stockholm, Sweden, and †School of Materials Science, University of Bradford, Bradford BD7 1DP, West Yorkshire, England

Received June 30, 1978

The phases occurring in samples of gross composition Ba_xWO_3 ($0.01 < x < 0.33$) heated at temperatures between 1073 and 1373°K have been determined using X-ray diffraction and electron microscopy. At all temperatures a tetragonal tungsten bronze phase with a narrow homogeneity range of $x = 0.20$–0.21 was observed to form. In addition, at temperatures up to 1273°K, a series of orthorhombic intergrowth bronzes forms within a restricted composition range around $x = 0.04$. The latter phases are unstable at higher temperatures and were not found in preparations made at 1323°K. Similarly a new type of bronze phase forms at $x = 0.14$–0.16 at temperatures up to 1323°K, but not at 1373°K. The structure of this phase is unknown. Aspects of the crystal chemistry of the barium bronzes and the relationships to other bronze phases are discussed.

Introduction

The formation of a barium tungsten bronze along the Ba_xWO_3 line has previously been reported by Conroy and Yokokawa (*1*). These authors reacted $BaCl_2$, WO_2, and WO_3 at temperatures in the interval 973–1273°K. An X-ray examination of the reaction products showed that a tetragonal tungsten bronze (TTB) similar to the tetragonal potassium tungsten bronze formed. This barium bronze appeared to have an extended homogeneity range from compositions close to WO_3 up to about $Ba_{0.13}WO_3$, under the conditions of synthesis employed in the reported study (*1*).

The TTB phase has been known to form with only four other metals in ternary M–W–O systems. The earliest of these to be known were with the electropositive alkali metals Na (*2*) and K (*2, 3*). These bronzes have extended homogeneity ranges along the A_xWO_3 line in the phase diagram and in the case of potassium, alkali contents close to the upper theoretical limit for interpolation of alkali atoms in the tunnels, $x = 0.60$, has been reported. Formally, no similar lower composition limit exists, but in practice the lowest limit of the composition range observed for the alkali TTB phases is found for sodium and is about $x = 0.26$. The far less electropositive metals lead and tin also form TTB phases. In the case of these two metals the lower limit of the homogeneity range has been found to be about $x = 0.18$ for lead (*4*) and 0.21 for tin (*5, 6*).

In the light of these findings the report that a TTB phase formed in the Ba_xWO_3 system at very low x values (*1*) seemed somewhat remarkable. Therefore we considered it worthwhile to reinvestigate the system. The results of the study are reported below and discussed in terms of the known crystal chemistry of other bronze phases.

0022-4596/79/050259-10$02.00/0

Experimental

The starting materials used were H_2WO_4 (Matheson, Coleman and Bell) and $BaCO_3$ (Merck, p.a.). WO_3 was prepared by heating H_2WO_4 in air at about 1100°K for several days, and WO_2 was prepared from the trioxide by reduction in a stream of H_2/H_2O gas mixture at 1023°K. To obtain a suitable partial pressure of water the hydrogen gas was allowed to bubble through water kept at a temperature of 358°K. The tungsten oxides were checked by X-ray powder diffraction, and the dioxide was also checked by careful weighing before and after reduction. Barium tungstate was prepared from appropriate mixtures of tungsten trioxide and barium carbonate by heating in a Pt crucible for three days at 1273°K.

Appropriate amounts of the metal tungstate, WO_2 and WO_3 were thoroughly mixed and sealed in evacuated silica tubes and normally heated at temperatures in the interval 1073–1273°K. A series of samples were also heated at 1323 and 1373°K to check the high-temperature stability of the ternary barium tungsten bronzes. The heating times ranged from one week to one month. Particular attention was payed to the region near to WO_3, and the majority of the samples had gross compositions lying upon the M_xWO_3 line of the phase diagram. In addition, a small number of samples were prepared at other gross compositions to clarify some aspects of the phase relations. After the heat treatment, all samples were quickly removed from the furnace, but no particular precautions were taken to quench them especially rapidly.

All samples were investigated by recording their X-ray powder patterns at room temperature with a Guinier–Hägg focusing camera using strictly monochromatic Cu$K\alpha_1$ radiation and KCl ($a = 0.6292$ nm) as an internal standard. The positions of the lines on the film were determined either visually or by means of an automatic Abrahamsson film scanner (7). Evaluation of the film data and indexing and refinement of unit cell parameters by least-squares techniques were performed on an IBM 1800 computer, using programs written by Brandt and Nord (8). In addition many samples were studied optically using a Zeiss Ultraphot microscope, and selected samples were examined in a JEM 100B electron microscope operating at 100 kV and fitted with a goniometer stage. Electron microscope specimens were prepared by crushing in an agate mortar under *n*-butanol and allowing a drop of the resultant suspension to dry on a net-like carbon film (*9*).

Results

The results obtained by X-ray diffraction were in accord with those obtained by electron microscopy and made it possible to determine the phase relations in the Ba–W–O ternary system for the composition region near to WO_3 and the temperature range between 1073 and 1373°K. In general very little difference could be detected between the samples heated for one week and those heated for one month, with the exception that prolonged heating times caused the diffraction lines on the X-ray powder diagrams to become sharper in the orthorhombic intergrowth region (see below). It appears, therefore, that the reaction proceeds fairly rapidly at the heating temperatures employed and that the phases produced do not decompose at a significant rate over this time scale. The results of these studies are summarised on the diagram shown as Fig. 1. Some aspects of the diagram and the results are presented in more detail below.

The TTB Phase

In agreement with the report of Conroy and Yokokawa (*1*) a ternary oxide of the TTB structure type was identified. This phase formed at all the temperatures studied, that is, between 1073 and 1373°K. However

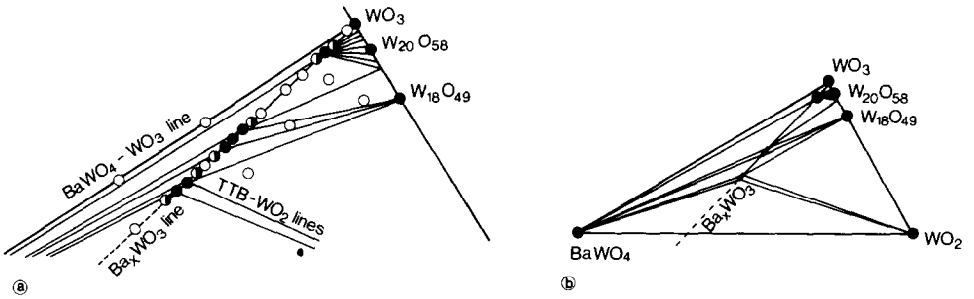

FIG. 1. (a) A part of the Ba–W–O phase diagram for temperatures between 1073 and 1273°K. The circles represent the gross compositions of the samples prepared. Filled circles correspond to preparations which were apparently monophasic according to powder X-ray diffraction, and half-filled circles represent those samples with only minor amounts of another phase present. (b) Phase diagram for the dioxide–trioxide region of the Ba–W–O system for temperatures between 1073 and 1273°K. In the binary tungsten–oxygen system the region between WO_3 and $WO_{2.875}$ can be regarded as containing more or less ordered *CS* oxides at any composition.

our findings for the homogeneity range were different from that reported by the latter authors, as the lower limit was found to be at about $Ba_{0.20}WO_3$ and the upper limit at about $Ba_{0.21}WO_3$. This is a very narrow homogeneity range and the compound approximates to a line phase. Consequently, calculations of the unit cell dimensions from samples of different overall compositions showed only a very small shift. Thus the lattice parameters of the tetragonal cell for the TTB phase found in the samples of overall compositions $Ba_{0.19}WO_3$ and $Ba_{0.22}WO_3$ were $a = 1.225 \pm 1$ nm, $c = 0.3810 \pm 3$ nm, and $a = 1.224 \pm 1$ nm, $c = 0.3818 \pm 3$ nm, respectively. The powder pattern for a bronze of composition $Ba_{0.21}WO_3$ is given in Table I.

Orthorhombic Intergrowth Phases

Within the temperature interval 1073–1273°K a series of previously unreported Ba_xWO_3 phases have been found. We shall refer to these as orthorhombic intergrowth bronzes for reasons which will be clear later. These phases were found in varying amounts in preparations of gross composition ranging from $Ba_{0.01}WO_3$ up to $Ba_{0.13}WO_3$, although the composition range over which they occurred alone is very narrow and near the value $x = 0.04$. The exact extension of this range is difficult to determine from the results obtained in this study, as the orthorhombic bronzes formed were disordered but the maximum extension seemed to fall within the interval $x = 0.03$–0.05.

The X-ray powder patterns obtained from the orthorhombic bronzes after annealing for 1 to 2 weeks were often weak and the lines were diffuse. Prolonged heating times caused the diffraction lines of the X-ray powder patterns to become somewhat sharper, indicative of either a higher degree of ordering or alternatively a growth of the structural regions within the crystals. In spite of this the latter patterns were difficult to index as they were made up of the superimposition of the individual patterns of more than one member of the orthorhombic bronze series. It might therefore be possible that these structures may not be true equilibrium products. A more extensive phase analysis over wider ranges of preparation conditions, to reveal the composition ranges for the different orthorhombic bronze structures and their long-time stability, will be needed to clarify this aspect.

The structures of these bronzes are very similar, as indicated by the electron microscopy results given below, and the main

TABLE I

THE POWDER X-RAY DIFFRACTION PATTERN OF THE TETRAGONAL TUNGSTEN BRONZE (TTB) PHASE FOUND IN A SAMPLE OF GROSS COMPOSITION $Ba_{0.21}WO_3$[a]

d_{obs} (nm)	I_{obs}	F^2_{obs}	$\sin^2\theta_{obs}$ ($\times 10^5$)	hkl	Δ[b]
0.8666	44	6	790	110	−1
0.5471	353	137	1982	210	+5
0.4328	155	99	3167	220	+3
0.3872	1240	1016	3958	310	+3
0.3815	1631	1378	4076	001	+7
0.3394	1065	1160	5150	320	+9
0.3238	194	234	5658	201	+7
0.3130	343	440	6055	211	+9
0.3059	78	106	6341	400	+13
0.2970	1407	2050	6727	410	+4
0.2886	345	535	7124	330	+5
0.2863	270	426	7237	221	+4
0.2738	648	1127	7915	420	+5
0.2718	1395	2463	8034	311	+10
0.2538	921	1887	9209	321	−1
0.2449	15	33	9889	430	+2
0.2389	208	485	10398	401	+1
0.2345	364	884	10791	411	−1
0.2101	132	405	13439	530	−7
0.2062	24	76	13946	431	−10
0.19528	35	124	15542	521	+4
0.19369	387	1406	15815	620	−4
0.19094	1064	3979	16274	002	−2
0.18256	379	1551	17801	630	+4
0.18029	119	499	18253	212	0
0.17471	43	192	19436	222	−3
0.17320	995	4518	19778	710	+4
0.17275	693	3163	19881	621	−7
0.17121	848	3937	20239	312	+9
0.16646	484	2369	21412	322	−5
0.16472	431	2150	21867	631	+2
0.16201	44	226	22603	402	0
0.16062	837	4371	22997	412	−2
0.15925	190	1007	23393	332	−1
0.15773	902	4863	23846	711	+3
0.15663	367	2002	24182	422	−3

[a] Refinement of the tetragonal lattice parameters gave $a = 1.2248 \pm 1$ nm, $c = 0.3819 \pm 1$ nm.

[b] $\Delta = 10^5 \times (\sin^2\theta_{obs} - \sin^2\theta_{calc})$.

differences occur along the a axis, whereas the b and c axes are almost the same. This was clearly reflected in the X-ray powder patterns, where the reflections with indices $(0, 2k, l)$ were found to be fairly sharp and among the strongest in the patterns. The d values for these lines did not vary much from one sample to another, regardless of preparation time or composition, again confirming that the b and c axes of the different bronze structures do not vary significantly, being of the order $b = 0.732$ nm and $c = 0.288$ nm. An example of a typical X-ray powder pattern obtained from a sample of overall composition $Ba_{0.04}WO_3$ is given in Table II.

In the electron microscope crystal fragments which were of the orthorhombic intergrowth type were easily recognized. The diffraction patterns were similar to those in the tin and lead systems which contain intergrowth faults, and typical examples are shown in Fig. 2. They are characterized by an approximately cubic subcell of strong reflections, one direction of which is subdivided further by superlattice reflections. In disordered fragments these reflections may be drawn out into continuous streaks while in more ordered crystal flakes approximately every nth superlattice spot is intense and coincides with a subcell reflection. We have taken this direction to coincide with the a axis of these phases and each member of the series is characterized by the n value taken from the diffraction pattern. As X-ray diffraction has shown the b and c axes to be normal to the a axis, the phases have an overall orthorhombic symmetry.

In the samples studied, with overall compositions lying between $Ba_{0.01}WO_3$ and $Ba_{0.15}WO_3$, the only n values encountered were those lying between 8 and 13. It would seem likely that this range will be extended by a more thorough examination of samples, particularly those prepared at temperatures other than those used in our studies. The spread of n values found in samples heated for two weeks or four weeks at 1273°K were not significantly different from each other and do not merit display in the form of histograms. It was found that one n value

TABLE II

THE POWDER X-RAY DIFFRACTION PATTERN OF THE ORTHORHOMBIC INTERGROWTH TUNGSTEN BRONZE (ITB) FOUND IN A SAMPLE OF OVERALL COMPOSITION $Ba_{0.04}WO_3$[a]

d_{obs} (nm)	I_{obs}	F^2_{obs}	$\sin^2\theta_{obs}$ ($\times 10^5$)	$\sin^2\theta_{calc}$ ($\times 10^5$)	hkl_{calc}
0.4125	24	17	3486		
0.4070	285	211	3581	3571	700
0.3885	1590	1302	3931	3939	001'
0.3791	31	26	4128		
0.3743	51	45	4235	4231	201
0.3664	1596	1483	4419	4428	020
0.3632	175	165	4497	4501	120
0.3569	1503	1485	4658	4664	800
0.3557	285	283	4689	4678	710
0.3416	108	116	5086	5084	320
0.3339	27	30	5320	5337	211
0.3318	23	26	5390		
0.3256	49	58	5598	5594	420
0.3180	56	70	5865		
0.3129	97	126	6061		
0.3090	576	772	6213	6212	411
0.3054	31	42	6362		
0.3025	25	35	6483		
0.2940	15	22	6863	6868	511
0.2899	122	187	7061	7051	620
0.2864	64	101	7234		
0.2828	26	42	7418		
0.2809	116	191	7521	7510	701
0.2767	25	42	7750		
0.2721	409	722	8012	7999	720
0.2663	1026	1897	8364	8367	021
0.2625	916	1748	8611	8603	801
0.2553	799	1619	9105	9092	820
0.2496	36	76	9525	9533	421
0.2412	73	167	10194	10189	521
0.2350	14	33	10747		
0.2343	21	51	10811		
0.2322	67	166	10998	10990	621
0.2170	16	45	12602	12586	630
0.2133	598	1778	13042	13031	821
0.2086	14	43	13636		
0.2024	7	23	14478		
0.2015	30	100	14611	14627	830
0.2003	72	244	14783		
0.19954	29	99	14901	14923	1220
0.19842	215	743	15069	15068	431
0.19411	287	1038	15745	15756	002
0.19276	8	29	15967		
0.18987	258	976	16456		
0.18712	24	93	16944	16935	112
0.18304	836	3408	17707	177011	040

[a] The sample is not monophasic. Studies of a great number of crystal fragments by electron microscopy showed that about two-thirds of these are of the 8-type ITB phase and the remaining have n values of 9- or higher. The calculated data in the table refer to an 8-type structure where the orthorhombic unit cell has the dimensions $a = 2.853$ nm, $b = 0.732$ nm, $c = 0.388$ nm.

tended to predominate with $n \pm 1$ or $n \pm 2$ present in lesser amounts.

Images of the crystal flakes of the orthorhombic intergrowth type were made using beams out to a distance corresponding to an interplanar spacing of about 0.2 nm. These showed the crystals to be divided up by a series of planar faults which were more or less disordered depending upon the crystal fragment examined. These crystals can equally well be thought of as consisting of lamellae of varying thicknesses of intergrowth bronzes united along planar boundaries. The faults or planar boundaries lie parallel to (100) planes in the crystal. Figure 3 shows an example of a fairly well ordered flake with the diffraction pattern corresponding to $n = 11$, shown in Fig. 2a.

Intuitive interpretation of such images directly in terms of structure must be made with caution, but even so, such images can confidently be taken to show that the structure of these phases is likely to consist of lamellae of a WO_3-like matrix of corner-sharing WO_6 octahedra, united along (100) planes. The latter planes may contain tunnels, but in such a case it is necessary to carefully compare computed images with those obtained experimentally before a precise structural model may be proposed. This will be reported at a later date.

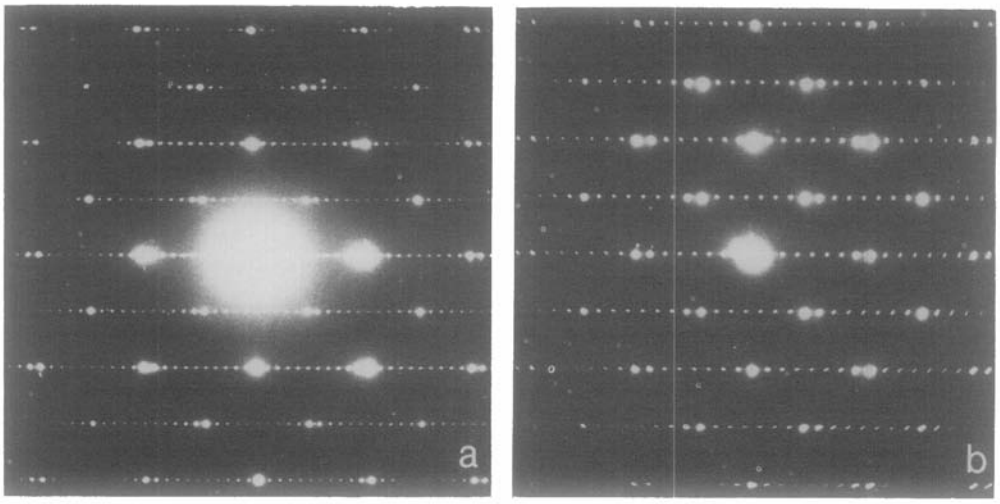

FIG. 2. Electron diffraction patterns from well-ordered orthorhombic intergrowth bronze crystal fragments, (a) with $n = 11$ and (b) with $n = 8$. The array of more intense spots corresponds to the WO_3 subcell reflections, while the closely spaced superlattice spots are parallel to the a^* axis of the orthorhombic cell.

On rare occasions crystal fragments were found in which the planar faults were very disordered, as shown in Fig. 4. In this case the crystals resemble WO_3 containing planar defects. These suggest that materials heated for short times or at lower temperatures might show a continuous change in microstructure from WO_3, through WO_3 containing random faults, to ordered intergrowth bronze structures.

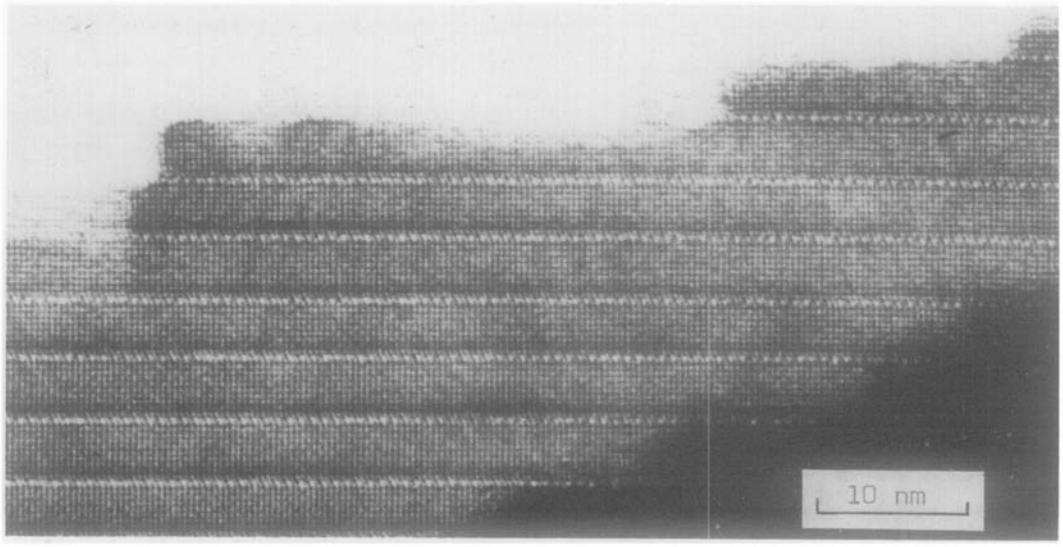

FIG. 3. High-resolution electron micrograph of a fragment of a crystal of an orthorhombic intergrowth tungsten bronze. The diffraction pattern of this fragment is shown in Fig. 2a.

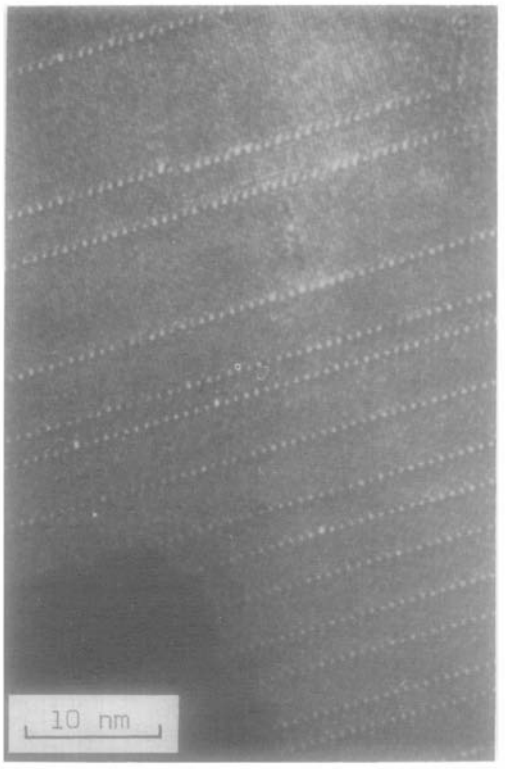

FIG. 4. Medium-resolution electron micrograph of a crystal fragment containing disordered faults of the type found in the orthorhombic intergrowth phases.

Other Phases

The X-ray diffraction analysis also showed that another type of bronze structure formed within the narrow composition interval $Ba_{0.14}WO_3$–$Ba_{0.16}WO_3$ at temperatures up to 1323°K. Electron diffraction studies provided information on the approximate dimensions of the orthorhombic unit cell, which made it possible to index the X-ray powder pattern of this phase, which is listed in Table III. No significant shifts can be seen in the lattice parameters of this phase in preparations made at overall compositions on both sides of the extension range. At present the structure of this phase is unknown.

In addition, no significant amounts of barium seem to substitute for tungsten in the binary tungsten oxides. For preparations made at the gross compositions $(Ba_{0.03}W_{0.97})_{18}O_{49}$ and $(Ba_{0.05}W_{0.95})O_2$ other oxides were clearly present and no shifts in the lattice parameters could be detected for the $W_{18}O_{49}$ and WO_2 oxides found in these preparations compared with the binary oxides themselves. Similarly a sample with an overall composition $(Ba_{0.45}W_{0.55})O_2$ showed that $BaWO_4$ might be looked upon as having no or only a narrow extension range along the dioxide line. The dioxide–trioxide region of the Ba–W–O phase diagram can thus be summarized as in Fig. 1b.

Discussion

The Ba–W–O system has been shown to support three bronze structure types, the orthorhombic ITB phases, the $Ba_{0.15}WO_3$ phase and the TTB phase. These materials bear a considerable resemblance to those found in the Sn–W–O (*5, 6*) and Pb–W–O (*4*) systems and to a lesser extent to the ITB phases of Hussain and Kihlborg found in the K–, Rb–, Cs–, and Tl–W–O systems (*10*). It is therefore of some interest to attempt to rationalize this behavior from a crystal chemical standpoint.

One of the most widely used crystallographic parameters is ionic size. There is no doubt that simple geometrical reasons such as the ternary metal ion size and the available space for this ion in the different bronze structure frameworks have a great influence on the structure type that actually is found to form for any ternary metal ion (*11*). Thus we can generally say that bronze-forming elements with an ionic radius of less than approximately 0.1 nm always yield a perovskite bronze, while for somewhat larger ions, the TTB structure type becomes favored and the largest ions prefer the HTB structure.

In Table IV we have listed all the metal ions which are known to form either TTB or HTB bronzes (*12, 13*). For comparative purposes we have listed the nominal ionic

TABLE III

THE POWDER X-RAY DIFFRACTION PATTERN OF THE ORTHORHOMBIC PHASE OBSERVED MONOPHASIC IN A SAMPLE OF GROSS COMPOSITION $Ba_{0.15}WO_3$[a]

d_{obs} (nm)	I_{obs}	F^2_{obs}	$\sin^2\theta_{obs}$ ($\times 10^5$)	hkl	Δ_b
0.6654	43	11	1340	110	−8
0.4426	175	108	3028	200	−2
0.4368	654	416	3109	120	−8
0.4056	358	267	3606	210	−14
0.3800	1671	1435	4107	001	−7
0.3490	169	174	4871	101	0
0.3318	865	997	5389	220	−1
0.3302	92	106	5443	111	−18
0.3128	996	1301	6062	130	−5
0.3027	204	286	6475	021	+2
0.2951	219	324	6812	300	−6
0.2882	278	434	7143	201	−1
0.2863	770	1218	7238	121	+7
0.2830	309	501	7409	310	+1
0.2770	494	839	7734	211	0
0.2543	43	87	9173	320	−5
0.2507	137	291	9437	040	−1
0.2497	443	941	9516	221	+13
0.2414	704	1609	10184	131	+4
0.2329	206	508	10941	301	+9
0.2268	79	206	11536	311	+14
0.2212	24	63	12123	400	+2
0.2181	83	235	12473	240	+5
0.2112	29	88	13299	321	+8
0.2093	10	30	13538	041	−14
0.2035	113	370	14321	141	+12
0.2024	76	252	14481	420	0
0.2004	20	67	14767	050	+20
0.19565	153	544	15499	150	−6
0.19114	56	209	16238	331	−3
0.18981	977	3702	16467	002	+13
0.18917	93	240	16578	241	−4
0.18777	16	62	16826	411	+1
0.18441	345	1385	17445	430	+15
0.18272	193	789	17769	250	−8
0.17862	38	163	18595	421	+1
0.17708	95	413	18920	500	−20
0.17398	547	2464	19601	151	−17
0.17191	179	825	20075	212	0
0.16718	252	1224	21226	060	−10
0.16590	749	3692	21556	440	−3
0.16470	727	3632	21870	251	−21
0.16227	615	3156	22529	132	+8
0.16041	139	728	23057	501	+4
0.15963	131	692	23281	302	+8
0.15837	18	56	23652	511	+9
0.15775	222	1198	23839	312	−23
0.15636	75	411	24265	260	−1
0.15475	14	78	24772	232	−22
0.15364	220	1250	25341	061	−8
0.15301	286	1642	25674	441	+1
0.15135	61	352	25899	042	+7
0.15072	32	186	26115	161	+8

[a] Refinement of the orthorhombic unit cell gave $a = 0.8849 \pm 1$ nm, $b = 1.0029 \pm 1$ nm, $c = 0.3798 \pm 1$ nm.
[b] $\Delta = 10^5 \times (\sin^2\theta_{obs} - \sin^2\theta_{calc})$.

radius of the ions for octahedral coordination taken from Shannon and Prewitt's compilation (*14*). There is some uncertainty about the radii of ions possessing lone pairs of electrons, such as Sn^{2+} and Pb^{2+}, and the figures quoted should be treated as approximate ones to reveal the overall crystal chemical trends only.

Consideration of Table IV then shows that ions with octahedral radii between about 0.1 and 0.138 nm form TTB bronzes. As Ba^{2+} falls within this region the existence of a TTB phase is therefore to be expected. It is noticeable that K^{1+}, with a radius of 0.138 nm, supports both the TTB structure and the HTB structure, and so is clearly a borderline ion from a geometrical standpoint. As Ba^{2+} is not far removed from K^{1+} in size it is possible that changed reaction conditions could move this ion into a borderline position. In particular synthesis under high pressure might result in the formation of HTB structure Ba_xWO_3 bronzes. This possibility is supported by the study of Gier *et al.* (*15*). They found that under the enhanced pressures obtaining during hydrothermal reaction hexagonal Li_xWO_3, $(NH_4)_xWO_3$, and Sn_xWO_3 bronzes formed, rather than the expected perovskite or TTB bronze structures. At higher pressures even

TABLE IV

TERNARY TUNGSTEN OXIDE SYSTEMS M_xWO_3 THAT FORM A TETRAGONAL (TTB) HEXAGONAL (HTB), OR INTERGROWTH (ITB) TUNGSTEN BRONZE[a]

TTB				
Ternary *M*-metal ion	Ionic radius (Å)	Composition range	o-rh ITB formation	Ref.
Na^{1+}	1.02	0.26–0.35	No	(*2*)
Pb^{2+}	1.18	0.18–0.35	Yes	(*4*)
Sn^{2+}	1.22	0.21–0.29	Yes	(*5, 6*)
Ba^{2+}	1.36	0.20–0.21	Yes	This paper
K^{+1}	1.38	0.40–0.59	No	(*2, 3, 10*)
HTB				
Ternary *M*-metal ion	Ionic radius (Å)	Composition range	hex ITB formation	Ref.
K^{1+}	1.38	0.13–0.31	Yes	(*10, 18*)
Rb^{1+}	1.49	0.13–0.33	Yes	(*10, 19*)
Cs^{1+}	1.70	0.13–0.32	Yes	(*10, 20*)
In^{1+}	(1.32)	0.2–0.33	Unknown	(*21, 23*)
Tl^{1+}	1.50	0.13–0.30	Yes	(*10, 22*)

[a] The ionic radii are for CN **VI** from Shannon and Prewitt (14) and are listed for comparative purposes only.

Na_xWO_3 has been found to adopt the HTB structure (*16*). Similar experiments with Ba_xWO_3 bronzes to check whether an HTB bronze could be prepared would therefore be of some interest.

Between the TTB and HTB bronzes and WO_3 there is a considerable stoichiometry range, which seems to be partly filled by a group of materials now known as intergrowth tungsten bronzes (ITB). In Table IV the M_xWO_3 systems that form either a HTB or a TTB phase are listed and it is obvious that the orthorhombic ITB formation is closely connected to the occurrence of a TTB phase in a way similar to that in which the hexagonal ITB phase is linked to the HTB structure.

We will consider first the orthorhombic intergrowth bronzes found in the Ba_xWO_3 system and reported earlier in this paper. The exact structure of these phases is as yet unknown and is the subject of continuing study. However, it is clear from the electron micrographs that the basic structure consists of lamellae of WO_3-like structure *n* octahedra wide united along fault planes with a so far unresolved structure which lie on planes parallel to {001} of WO_3. We presume that the Ba atoms or ions are located in these fault planes. These phases show a considerable similarity to orthorhombic intergrowth bronzes in the Sn- and Pb–W–O systems (*4–6*), and it is possible that the structures of these phases are the same from one ion to the next, although this has yet to be confirmed by X-ray structure determination.

The hexagonal ITB phases formed by the larger ions shown in Table IV are analogous to the orthorhombic ITB phases formed by the smaller ions. In this case the structures of the ITB phases have been shown to be made up of slabs of WO_3 separated by rows of tunnels which are elements of the HTB structure itself (*10*). The structural economy of this method of accommodating small amounts of these large ions in the WO_3 matrix suggests that it will operate in all systems where a HTB phase forms. From this point of view hexagonal ITB phases would also be expected to form in the In–W–O system, and a reinvestigation of the In_xWO_3 bronzes would be of considerable interest.

The present phase analysis also allows us to comment on the superconductivity studies of Sweedler *et al.* (*17*). They found that a barium bronze of nominal composition $Ba_{0.13}WO_3$ became partly superconducting at 1.9°K. Our results suggest that their preparation was biphasic, containing orthorhombic ITB materials and a larger amount of either the TTB phase or the $Ba_{0.15}WO_3$ phase which we have found. It is most likely that the superconducting component in the preparation was the orthorhombic ITB part,

as the closely related tin TTB phase does not become superconducting, at least down to temperatures of 1.3°K (*15*), and Sweedler *et al.* also state that only the smaller fraction of their sample, some 35%, became superconducting. These results suggest that it would be of interest to test all the orthorhombic intergrowth bronzes so far found for superconductivity. These experiments are now under way and will be reported in the future.

Acknowledgments

One of the authors (R.J.D.T.) is grateful to the Science Research Council (London) for an equipment grant. The research has also been performed within a program supported by the Swedish Natural Science Research Council and T.E. is grateful to Professor Arne Magnéli for the experimental facilities put to his disposal.

References

1. L. E. CONROY AND T. YOKOKAWA, *Inorg. Chem.* **4**, 994 (1965).
2. J.-M. REAU, C. FOUASSIER, G. LE FLEM, J.-Y. BARRAUD, J.-P. DOUMERC. AND P. HAGENMULLER, *Rev. Chim. Miner.* **7**, 975 (1970).
3. L. KIHBORG AND A. KLUG, *Chem. Scripta* **3**, 207 (1973).
4. THOMMY EKSTRÖM AND R. J. D. TILLEY, *J. Solid State Chem.*, **24**, 209 (1978).
5. I. J. MCCOLM, R. STEADMAN, AND C. DIMBYLOW, *J. Solid State Chem.* **14**, 185 (1975).
6. THOMMY EKSTRÖM, M. PARMENTIER AND R. J. D. TILLEY. In preparation.
7. G. MALMROS AND P.-E. WERNER, *Acta Chem. Scand.* **27**, 493 (1973).
8. B. G. BRANDT AND A. G. NORD, *Chem. Commun. Univ. Stockholm*, No. V (1970).
9. J. R. GANNON AND R. J. D. TILLEY, *J. Microsc.* **106**, 59 (1976).
10. A. HUSSAIN AND L. KIHLBORG, *Acta Cryst.* A **32**, 551 (1976).
11. THOMMY EKSTRÖM AND R. J. D. TILLEY, to be published.
12. P. HAGENMULLER, *Compreh. Inorg. Chem.* Vol. 4, Ed. J. C. Bailar *et al.* Pergamon Press, Oxford 1973.
13. P. G. DICKENS AND P. J. WISEMAN, M. T. P. *Int. Rev. Sci., Inorg. Chem.*, p. 211. Series 2, Vol. 10 (L. E. J. ROBERTS, ed.), Butterworths, London (1975).
14. R. D. SHANNON AND C. T. PREWITT, *Acta Cryst.* B **35**, 925 (1969).
15. T. E. GIER, D. C. PEASE, A. W. SLEIGHT, AND T. A. BITHER, *Inorg. Chem.* **7**, 1646 (1968).
16. T. A. BITHER, J. L. GILLSON, AND H. S. YOUNG, *Inorg. Chem.* **5**, 1559 (1966).
17. A. R. SWEEDLER, J. K. HULM, B. T. MATTHIAS, AND T. H. GEBALLE, *Phys. Lett.* **19**, 82 (1965).
18. E. BANKS AND A. GOLDSTEIN, *Inorg. Chem.* **7**, 966 (1968).
19. D. R. WANLASS AND M. J. SIENKO, *J. Solid State Chem.* **12**, 362 (1975).
20. A. MAGNÉLI, *Acta Chem. Scand.* **7**, 315 (1953).
21. R. J. BOUCHARD AND J. L. GILLSON, *Inorg. Chem.* **7**, 969 (1968).
22. P. E. BIERSTEDT, T. A. BITHER AND F. J. DARNELL, *Solid State Commun.* **4**, 25 (1966).
23. A. B. SWANSON AND J. S. ANDERSON, *Mat. Res. Bull.* **3**, 149 (1968).